33rd Annual International Conference of the IEEE EMBS
Boston, Massachusetts USA, August 30 - September 3, 2011

CMRI Based 3D Left Ventricle Motion Analysis on Patients with Acute Myocardial Infarction

H. Gao, K. Kadir, C. Berry, A. Payen, J. Soraghan, X. Luo

Abstract—**3D Quantitative measurement of left ventricle (LV) motion on patients with acute myocardial infarction has been recognized as essential for effective LV function diagnosis. This paper presents a method to quantify 3D LV motion obtained from conventional CINE MRI using image analysis based on mathematical modeling. Level set method is employed for segmentation, and a 3D LV geometry was reconstructed by co-registering different views of MRI images. A mathematical model of LV geometry was then constructed to quantitatively describe the LV wall inward motion. The results using real data show that the method is able to quantify the LV inward motion, and can clearly represent the changed motion pattern with the follow-up data. Furthermore, the LV motion analysis for 8 patients with acute myocardial infarction (MI) show that high inward motion occurs mainly in the basal region of LV while a negative relation is found between LV ejection fraction (EF) improvement after acute MI and solely basal region inward motion, which could be helpful for diagnosis and LV EF recovery prediction.**

I. Introduction

Qualitative analysis of the motion of left ventricle (LV) in patients with acute myocardial infarction (MI) has become a standard practice in clinical cardiology [1, 2]. It has been found that an abnormal LV wall motion is closely related to the presence and severity of coronary artery disease [3]. LV wall motion analysis using 2D/3D Echocardiography, and cardiac MRI [4, 5] has been recognized an essential parameter for diagnosis of heart function. A study [5] has been carried out to investigate the relationship between quantitative 3D LV wall motion and regional ischemia with real-time ultrasound volume imaging from canine left ventricle. The results suggested that parameters from wall motion may be reasonable candidates in identifying and quantifying acute regional ischemia in patients.

Although quantitative wall motion assessment might improve the diagnostic procedure and decision making, this is not usually carried out by clinicians due to technical difficulties. The first essential step involved in motion analysis is to accurately delineate myocardial wall boundaries. Much research has been devoted into the segmentation of myocardial wall based on CINE MRI data including level sets method [6], shape and appearance model [7]. However there is no established standard and reliable way for segmenting Cardiac MR Images. The segmentation accuracy varies according to the image quality and segmentation methods. The second step is how to mathematically characterize LV motion, and link these with the pathological states of LV.

Since LV wall motion is closely related to myocardial injury, some patterns of LV wall motion after acute MI may provide predictions of future LV status, such as LV function recovery. In the paper we will develop a method for 3D quantitative LV wall motion analysis from CINE MRI (image based modeling). This will then allow an investigation of the possible relationship of LV motion pattern just after acute MI and LV ejection fraction (EF) improvement with 3 months follow up study to be carried out. The remainder of the paper is organized as follows. In Section 2, Myocardial LV wall segmentation and inward motion model are introduced. In secton 3, detailed inward motion pattern with patients are analyzed. Discussion and conclusions are provided in Section VI and V.

II. Methods

Three main stages are involved in the development of LV wall motion analysis framework namely

(1) stage 1: the cardiac MR image acquisition;

(2) stage 2: MR image processing, i.e. the segmentation of LV wall;

(3) stage 3: mathematical modeling of LV geometry and motion quantification.

A. Cardiac MRI Acquisition of LV

Cardiac MRI was performed on 8 patients with heart attack resulting from blockage in the left anterior descending (LAD) coronary artery. The first MRI scan was performed within 2 days following an acute MI on a Siemens Magnetom Avanto (Erlangen, Germany) 1.5 Tesla scanner with an 8-element phased array cardiac surface coil. A follow-up Cardiac MRI scan was performed after 3 months of the acute MI. The study protocol was approved by the local ethics committee and all patients gave written informed consent. Conventional CINE MRI sequence was applied for each patient: flip angle 80°, echo time=1.12ms, bandwidth=930Hz/pixel, slice thickness= 8mm. All images were stored in the DICOM format. The basic information

Manuscript received March 31, 2011. This work was supported by a project grant from Chief Scientist Office, Scottish Government

H. Gao is with BHF Glasgow Cardiovascular Research Center, University of Glasgow, UK G12 8TA, and the Centre for excellence in Signal and Image Processing (CeSIP), University of Strathclyde, Glasgow, UK, G1 1XW (email: hao.gao@eee.strath.ac.uk)

K. Kadir is with Centre for excellence in Signal and Image Processing (CeSIP), University of Strathclyde, Glasgow, UK, G1 1XW (email: kushsairy@eee.strath.ac.uk)

C. Berry is with BHF Glasgow Cardiovascular Research Centre, University of Glasgow, Glasgow, UK, G12 8TA(email: colin.berry@glasgow.ac.uk, phone: 44(0) 141 211 6311)

A. Payen is with Golden Jubilee National Hospital, Clydebank, UK, G81 4HX(email: alex.payne@nhs.net)

J. Soraghan is with Centre for excellence in Signal and Image Processing (CeSIP), University of Strathclyde, Glasgow, UK, G1 1XW (email: j.soraghan@eee.strath.ac.uk)

X.Luo is with School of Mathematics and Statistics, University of Glasgow, Glasgow, UK, G12 8QW(email: Xiaoyu.luo@glasgow.ac.uk)

including EF for the 8 patients are summarized in Table I.

Table I. Patient Information (EF: Ejection Fraction)

Patient	Age	Gender	EF after Acute MI	EF (3months later)
S1	55	F	48.3%	64.3%
S2	50	M	38.8%	51.8%
S3	41	F	39.6%	58.3%
S4	60	M	26.9%	64.9%
S5	49	M	49.1%	49.7%
S6	28	M	31.3%	37.8%
S7	51	M	37.7%	45.2%
S8	50	F	37.2%	29.9%

Diabetes: 1/8; Previous MI: 0; Previous percutaneous coronary intervention: 0; Drug therapy with aspirin (8/8), clopidogel(8/8), beta blocker (5/8); angiotensin converting enzyme inhibitor (5/8). Healthy subjects typically have EF between 50% to 65%.

B. LV Boundary Segmenation

1) Basis of variational level set method: Variational level set method (VLSM) without-re-initialization [8] was used for LV segmentation. The evolution equation of the traditional level set formulation can be written in the following general form,

$$\frac{\partial \phi}{\partial t} + F\left|\nabla \phi\right| = 0 \tag{1}$$

where F is the speed function, which depends on the imaging data I and level set function ϕ. The moving front C can be represented by the zero level set as

$$C(t) = \{(x, y) \mid \phi(t, x, y) = 0\} \tag{2}$$

In this study, C represents the endocardial and epicardial boundaries of the LV.

For the traditional LSM, ϕ is required to be kept close to a signed distance function during the evolution, therefore re-initialization is required constantly. However the re-initialization procedure can be very complicated and time consuming, and has significant side effects [9]. In order to overcome those difficulties, the evolution (1) is redefined as

$$\frac{\partial \phi}{dt} + \frac{d\omega}{d\phi} = 0 \tag{3}$$

where ω is

$$\omega(\phi) = \underbrace{\alpha \int_\Omega \frac{1}{2}(\left|\nabla \phi\right| - 1)^2 dxdy}_{the\ first\ \ term} + \underbrace{\beta \int_\Omega g\delta(\phi)\left|\nabla \phi\right| dxdy}_{the\ second\ \ term} + \underbrace{\gamma \int_\Omega gH(-\phi)dxdy}_{the\ third\ \ term} \tag{4}$$

The first term in the right hand side of Equation 3 is the measurement of the distance of ϕ to a signed distance function, which will eliminate the re-initialization of ϕ during level set evolution, and α >0. The second and third terms in the right hand side of Equation 3 are the energy terms which will drive the motion of the zero level curve of ϕ to the desired boundaries. $\beta > 0$ and γ is a constant. δ is the univariate Dirac function and H is the Heaviside function. g is the edge indicator, defined as

$$g = \frac{1}{1 + \left|(\nabla G_\sigma) * I\right|^2} \tag{5}$$

G_σ is the Gaussian kernel with standard deviation σ .

By using calculus of variation, the Euler-Langrange form of (3) can be derived, which was solved using finite difference methods in the study.

2) CINE MRI Segmentation With Short Axis Slices The above VLSM was implemented in Matlab. The segmentation procedure was carried out on a slice-by-slice basis as follows:

- Pre-processing MRI images, including (a) gray scale dilation operation for reducing papillary muscle; (b) A traditional anisotropic diffusion process to reduce the intensity heterogeneity;
- Endocardial boundary tracking by VLSM, followed by the convex hull algorithm to exclude papillary muscles;
- Initialization of VLSM for epicardial boundary segmentation by growing endocardial boundary outward slightly. The averaged LV wall thickness in septum region was assessed in order to apply constrain for epicardial boundary tracking, which will stop boundary leaking.
- Epicardial boundary tracking by VLSM

Fig.1 shows the endocardial and epicardial boundary segmentation by VLSM from base to apex, for a total of 7 images. It is noticed that the boundary detection in apex region was not as good as in basal region due to the presence of many trabeculae.

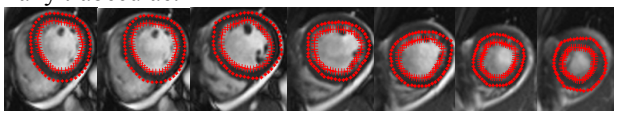

Fig.1. Endocardial and epcardial boundary detected by VLSM

3) 3D LV Boundary Data Assembly: The CINE MRI with 4-chamber view was selected for aligning endo/epi-cardial boundaries. Fig.2(a) shows the corresponding long axis CINE MRI images for Fig.1. The endocardial boundary in Fig.2(a) was manually traced by picking points individually. Two points in the basal region for mitral valve and one point in the apex were defined, indicated by *p1*, *p2* and *p3* in Fig.2(a). Then the ventricle axis can be defined as from the middle point of *p1* and *p2* to *p3*. The location and orientation for each short axis slice was available from the DICOM image. Fig.2(b) shows the aligned endo/epi-cardial boundaries in 3D, superimposed with 4-chamber view.

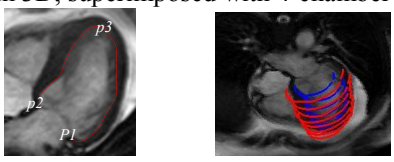

(a) (b)

Fig.2. (a): segmentation with 4-chamber view; (b) aligned endo/epi-cardial boundaries in 3D

C. LV Motion Analysis

1) LV Geometry Reconstruction: LV geometries at peak systole and diastole phases were reconstructed, as shown in Fig.3(a), represented by hexahedral meshes. Fig.3(b) shows the endocardium surface at systole (blue) and diastole (red) phases. From Fig.3(b), a penetration of blue surface through red surface can be identified, indicating the motion in the apex septum region was severely reduced due to MI.

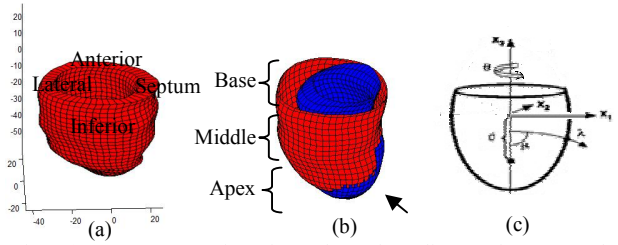

Fig.3. (a) 3D reconstruction of LV; (b) Endocardium surface at systole (blue) and diastole (red) phases; (c) prolate spheroidal coordinate system.

2) LV Motion Definition: From Fig.3, LV motion can be defined as the difference at endocardium surface between systole and diastole phases. In order to quantitatively measure the LV motion, a prolate spheroidal coordinate system was chosen to parameterize the LV geometry, which was shown to be able to provide an accurate and computationally efficient representation of the LV geometry [10], see in Fig.3(c). In the prolate spheroidal coordinate system, $\mu > 0$ represents the longitudinal angular coordinate, starting from the apex; θ is the circumferential angular coordinate, and $\lambda(\mu,\theta)$ represents the radial coordinate along an arc from the central axis. The shape and size of the surface with constant λ depend on the chosen focal length d. In this study, the focal length d was defined as [5]

$$d = \frac{2}{3}(\textit{the base to apex distance}) / \cosh(1) \qquad (6)$$

Then the endocardial surface data represented by Cartesian system (x_1, x_2, x_3) were fitted into the prolate spheroidal coordinate (λ, μ, θ). The hammer projection (cutting in the middle of septum region) was used to represent the LV surface, which converts the 3D LV surface into 2D representation. Once the parametric representations of the endocardial surface at end diastole and end systole were obtained, quantitative measurements of LV wall motion could be defined and applied to the patients. In the study, we defined the inward motion between end diastole and end systole as

$$\lambda_M = \lambda_{Diastole} - \lambda_{Systole} \qquad (7)$$

λ_M was presented with hammer projection in order to preserve the relative surface area.

III. Results

From Table I, patient 1 had recovered well according to the EF change (>50%). Fig.4(a) shows the contour of λ_M map with hammer projection just after acute MI. The reduced motion area is seen to be mainly located in the septum and apex regions, which was related to the diseased state of LV. Fig.4(b) shows the contour of λ_M for the same subject 3 months later after MI. The comparison shows that the whole LV can properly pump after three months in terms of EF.

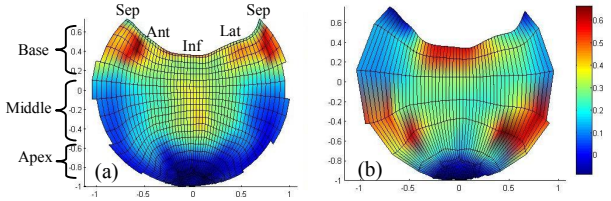

Fig.4. (a): λ_M for S1 right after acute MI; (b) λ_M for S1 3 months later after acute MI. Sep: Septum; Ant: Anterior; Inf: Inferior; Lat: Lateral.

We proceeded to calculate the λ_M maps for the 8 patients after acute MI, shown in Fig.5.

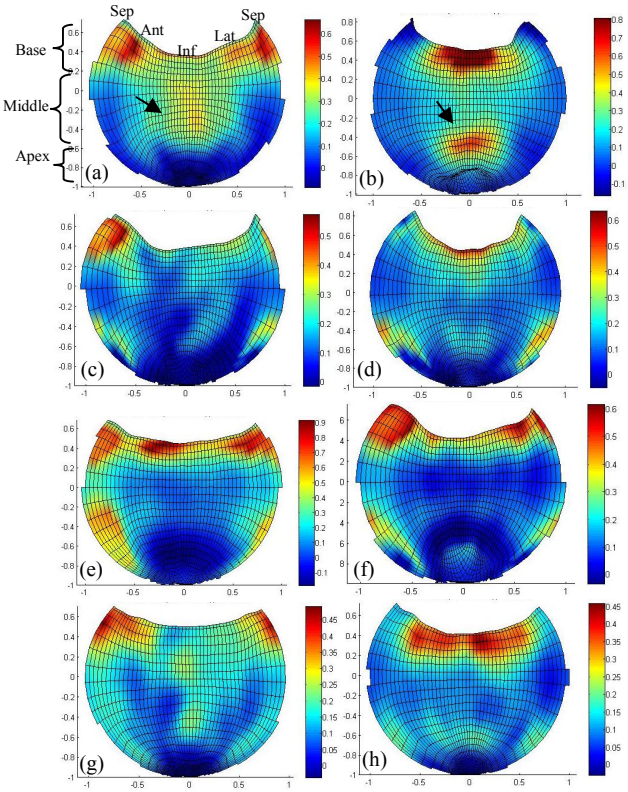

Fig.5. λ_M maps for the 8 patients from S1 to S8. A good inward motion away from the basal region is indicated by arrows in (a,b)

For the 8 studied patients, since the MI resulted from LAD coronary artery, the motion in the septum and apex (main infarct region) had been greatly impaired, which can be seen in Fig.5, where those regions show small or even negative values of λ_M. As a result, the LV of these patients attempts to compensate for the lack of motion from the apex region by allowing a greater motion in the basal region (hyper-dynamics), which also can be seen in Fig.5 (the red region at top for individual hammer map). Although MI resulted from the same coronary artery, the motion pattern after acute MI was different among the 8 patients. For S7 and S8, the high λ_M region is mainly located in the basal region, while the motion in the other regions was greatly

reduced. This was different from S1 and S2, where except for the basal region, regions such as the middle part still kept good inward motion, as indicated by arrows in Fig.5(a) and (b). For S3 and S4, the inward motion in the basal region was not significantly higher than other regions. S5 and S6 also showed higher inward motion in the basal region.

The first 3 slices (starting from LV base) was used to represent the LV basal region, and a cut-off value of λ_M was defined as half of the maximum λ_M from that patient to represent the hyper-dynamics region, then the total hyper-dynamics region in the whole LV (HW) and basal region (HB) can be calculated, the surface area was taken from the endocardium. A ratio between HW and HB is defined as R_{BW}=HB/HW, representing the relative hyper-dynamics region in the basal region. A value of 1 for R_{BW} indicates the hyper-dynamics is solely in the basal region. Fig.6 shows the scatter plot between R_{BW} and EF changes during 3 months for the 8 patients. A negative correlation is found within the 8 patients, with r=-0.6, p=0.1, indicating that the different inward motion pattern of λ_M in the basal region of diseased LV might be indicative for the longer term EF improvement.

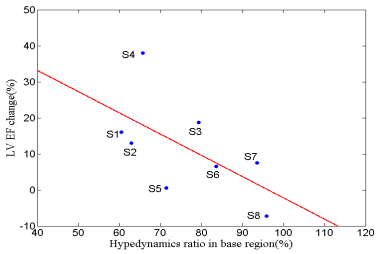

Fig.6 The scatter plot between R_{BW} and EF changes

IV. Discussion

With current MRI techniques, patients with acute MI can be scanned with high quality and resolution, which makes it a useful tool for diagnosis. In our work, the same patients were scanned twice, which provided an opportunity to investigate how patients recover over time. Visual analysis of LV motion from clinical imaging provides little quantitative information, and depends heavily on the experience of clinicians making it subject to high inter-observer variability. Therefore there is a need to develop methods for quantitative analysis of cardiac images in order to provide a more objective and accurate wall motion measurements for clinical diagnosis. In this study, a framework of quantifying LV motion from MR images was proposed, and applied to 8 patients.

Variational level set method was used for segmenting the LV geometry, which has allowed 3D LV geometry reconstruction from CINE MRI images. This approach has the potential for automation of the whole process, while reducing the inter-observer uncertainties. The imaging process method will make possible real-time 3D motion analysis on patients with acute MI. Another advantage of the study is that the 3D LV motion analysis was carried out by using CINE MRI, which is a basic standard imaging sequence for cardiac MRI, and used in routine clinical environment.

The comparison of the λ_M map among the 8 patients after acute MI shows that λ_M might be used for clinical diagnosis and treatment decision making. Patients with higher λ_M map solely in the basal region may be related to a greater immediate compensation of the decreased LV ejection after acute MI, which will influence the long term EF recovery. Indeed, Liu et al [11] found that more severely infracted LV could show stronger and longer basal contraction. Our result of the λ_M map is consistent with this observation. This is an interesting and potentially useful finding for clinical applications, while some other factors also affect the recovery procedure, such as infarction size. Therefore it remains to be confirmed and validated using a larger group of patients.

V. Conclusion

In this paper a method for 3D quantitative analysis of LV motion on patients with acute MI by integrating imaging analysis and mathematical modeling based on conventional CINE MRI was presented. The proposed method is capable of characterizing the reduced motion of diseased LV, and the significance of the basal region motion pattern is found to be associated directly with a possible poor LV ejection fraction improvement. Consequently the different LV motion pattern after acute MI may be helpful in diagnosis, and even recovery prediction.

References

[1] R.Y. Kwong, *Cardiovascular Magnetic Resonance Imaging*. Address: New Jersey, Humana Press Inc., 2008.

[2] N.B. Schiller, P.M. Shah and M. Crawford etc, "Recommendations for quantitation of the left ventricle by two-dimensional echocardiography. "*J. Am. Soc. Echocardiogr.*, vol. 2, pp. 358-367–25, 1989.

[3] A. Elhendy, DW. Mahoney and BK. Khandheria, etc,"Prognostic significance of the location of wall motion abnormalities during exercise echocardiography ", J. Am. Coll. Cardiol. vol. 40, pp. 1623-1629, 2002.

[4] S.L. Herz, T. Hasegawa, A.N. Makaryus, etc. . "*J*Quantitative three dimensional wall motion analysis predicts ischemic region size and location. " Annals of biomedical engineering vol.38, pp. 1367-1376, 2010

[5] S.L. Herz, C.M. Ingrassia and S. Homma, etc, "Parameterization of left ventricular wall motion for detection of regional ischemia". Annals of Biomedical Engineering, vol. 33, pp. 912-919, 2005

[6] N. Paragios, "A level set approach for shape-driven segmentation and tracking of the LV", IEEE Trans. Med. Imaging., vol. 22 (6) pp:773-776, 2003

[7] S. C. Mitchell et al., "Multistage hybrid active appearance model matching: segmentation of left and right ventricles in cardiac MR images, " IEEE Trans. Med. Imaging., vol. 20(5) pp. 415–423, 2001.

[8] C. Li, C. Xu, C. Gui, M. Fox, "Level set evolution without re-initialization: A new variational formulation". CVPR, 2005 PMF.

[9] J. Gomes and O. Faugeras, "Reconciling distance functions and level sets". J. Visual Communic. And Imag. Representation, vol. 11, pp. 209-223, 2000

[10] I.J. Nielsen, B.H. LeGrice, P.J Smaill, et al. "Mathematical model of geometry and fibrous structure of the heart". Am J Physiol Heart Circ Physiol, vol. 260, pp.H1365-H1378, 1991

[11] Y. Liu, H. Wen, R.C. Gorman, et al. "Reconstruction of myocardial tissue motion and strain fields from displacement-encoded MR imaging". Am J Physiol Heart Circ Physiol, vol. 297, pp. H1151-H1162, 2009